UNIVERSITAT POLITÈCNICA
DE CATALUNYA

Analysis and control of an hybrid system: a doubly-fed induction machine and a back-to-back converter.

Carles Batlle, Arnau Dòria-Cerezo, Enric Fossas

IOC-DT-P-2005-16
Setembre 2005

Institut d'Organització i Control
de Sistemes Industrials

Analysis and Control of an Hybrid System: a doubly-fed induction machine and a back-to-back converter.

Carles Batlle, Arnau Dòria-Cerezo and Enric Fossas
Universitat Politècnica de Catalunya

July, 2005

Abstract

This report describes the port interconnection of two subsystems: a power electronics subsystem (a back-to-back AC/AC converter (B2B), coupled to a phase of the power grid), and an electromechanical subsystem (a doubly-fed induction machine (DFIM), coupled mechanically to a flywheel and electrically to the power grid and to a local varying load). The B2B is a variable structure system (VSS), due to the presence of control-actuated switches; however, from a modelling and simulation, as well as a control-design, point of view, it is sensible to consider modulated transformers instead of the pairs of complementary switches. The port-Hamiltonian models of both subsystems are presented and, using a power-preserving interconnection, the Hamiltonian description of the whole system is obtained. Using passivity-based controllers computed in the Hamiltonian formalism for both subsystems, a closed loop Hamiltonian system is presented; simulations are run to test the correctness and efficiency of the Hamiltonian network modelling approach used in this work.

1 Introduction

The central paradigm of network modelling of complex systems is to have individual open subsystems with well defined port interfaces, hiding an internal model of variable complexity, and a set of rules describing how the subsystems interact through the port variables. One implementation of this general idea is what is known as port Hamiltonian systems or port-controlled Hamiltonian systems (PCHS) [11][12] (see also [7] and references therein). In this approach, energy plays a fundamental role, port variables are conjugated variables such that their product has dimension of power, and the interconnection of subsystems is implemented by means of what is called a Dirac structure, which enforces the preservation of power, and can be seen as a generalization of Tellegen's theorem of circuit theory [13]. PCHS theory allows the coupling of systems from different domains using energy as the linking concept, and provides the mathematical foundation for bond-graph modelling [5][8]. Although originally developed for lumped parameter systems, PCHS theory has been extended to distributed parameter systems as well [22].

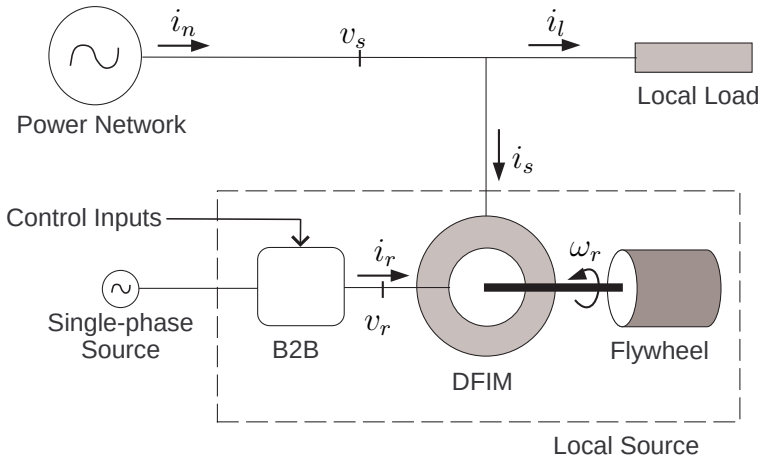

Figure 1: The system: A DFIM coupled to a flywheel connected between a local load and a power grid, controlled by a B2B converter.

Besides describing systems in a modular, scalable and non domain-specific way, PCHS theory allows the implementation of passivity-based control methods [10][21] in a natural way, using energy as the storage function [14]. The clear separation between (a) constitutive relations, given by the energy, or Hamiltonian, function, (b) the structure matrix, describing how energy flows inside the system, and (c) the power ports, some of which may be terminated by dissipative elements, allows the design of controllers with a clear physical interpretation in what is known as Interconnection and Damping Assignment Passivity-Based Control (IDA-PBC) [15].

In this report we concentrate on the modelling and simulation part of PCHS theory, although control results are presented in order to be able to run sensible simulations. The system under study is a complex one, made of a doubly-fed induction machine driven by a power converter and coupled to a mechanical flywheel, which has the general goal of compensating the active and reactive power of a local variable load connected to the power grid, using the flywheel as an energy reservoir.

Doubly-fed induction machines (DFIM) have been proposed in the literature, among other applications, for high performance storage systems [1], wind-turbine generators [16][19] or hybrid engines [6]. The attractiveness of the DFIM stems primarily from its ability to handle large speed variations around the synchronous speed (see [17] for an extended literature survey and discussion). In this work, we are interested in the application of DFIM as part of an autonomous energy–switching system that regulates the energy flow between a local prime mover (a flywheel) and the electrical power network, in order to satisfy the demand of a time–varying electrical load, see Fig. 1.

The Back-to-back (B2B) converter, connected to an auxiliary single-phase grid, provides the desired PWM rotor voltages to the DFIM. The B2B has the nice feature that power can flow in any direction. In particular, in our application the rotor energy of the DFIM can flow back to the converter for some operating conditions [3].

The global goal of the system is to supply the required power to the load with a high network power factor, *i.e.*, $Q_n \sim 0$, where Q_n is the network reactive power. Moreover, we require a unity power factor for the single-phase auxiliary grid and a constant value of the DC capacitor link of the B2B.

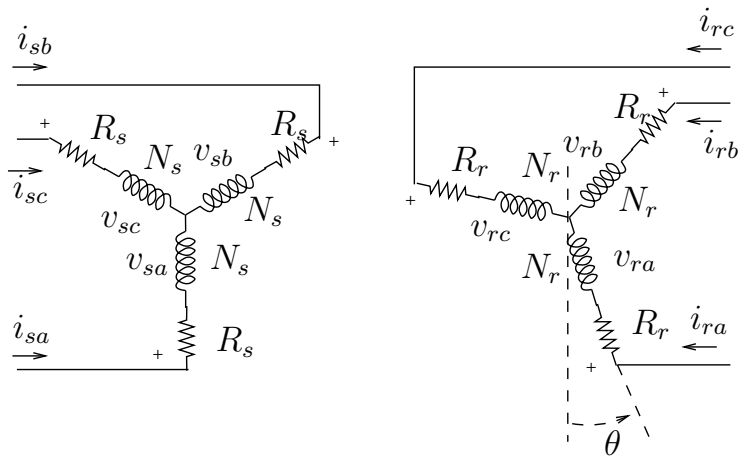

Figure 2: Basic scheme of the doubly-fed induction machine

This report is organized as follows. Section 2 presents the port Hamiltonian models of the several subsystems and their interconnection; in particular, the Dirac structures involved in the interconnection and some associated transformations are identified. Using these, a port Hamiltonian model of the full system is constructed. Section 3 reviews the control objectives as well as the controllers obtained elsewhere [2][3][4] using IDA-PBC. Section 4 displays simulations of the closed loop system for several operating conditions, and Section 5 states our conclusions.

2 Port-controlled Hamiltonian Models

In this section we recall the previous work presented in deliverable D 4.1.2 related to the Hamiltonian model of the system, which will be used in the controller design. Port-controlled Hamiltonian Systems (PCHS) describe, from an energetic point of view, a large kind of systems [7]. An explicit PCHS has the form

$$\begin{cases} \dot{x} = (\mathcal{J}(x) - \mathcal{R}(x))(\nabla H(x))^T + g(x)u \\ y = g^T(x)(\nabla H(x))^T \end{cases} \tag{1}$$

where $x \in \mathbb{R}^n$ are the energy variables, $H(x) : \mathbb{R}^n \to \mathbb{R}$ is the energy (or Hamiltonian) function, $u, y \in \mathbb{R}^m$ are the port variables, $\mathcal{J}(x) = -\mathcal{J}^T(x) \in \mathbb{R}^{n\times n}$ is the intra-connection structure matrix, describing how the energy flows inside the system, $\mathcal{R} = \mathcal{R}^T \geq 0 \in \mathbb{R}^{n\times n}$ is the dissipation matrix, and $g(x) \in \mathbb{R}^{n\times m}$ is the interconnection matrix, describing the port connection of the system to the outside world. Port variables are conjugated, so that $[u][y]$ has units of power. Non-negativeness of $\mathcal{R}$ ensures that the map $u \to y$ is passive [21].

2.1 The Doubly-fed Induction Machine coupled to a flywheel

Fig. 2 shows a scheme of a doubly-fed three-phase induction machine. It contains 6 energy storage elements, with their associated dissipations, and 6 ports (the 3 stator and the 3 rotor voltages and currents).

A Port-controlled Hamiltonian model of a DFIM coupled to a flywheel is given in [3]. This model is described in dq-coordinates [9], so that three-phase variables (abc) are reduced to two-phase variables (dq). The variables are (the D subindex refers to the DFIM subsystem) $x_D^T = (\lambda_s^T, \lambda_r^T, J_m\omega_r) \in \mathbb{R}^5$, or $x_D^T = (\Lambda^T, x_m)$, where $\Lambda^T = (\lambda_s^T, \lambda_r^T) \in \mathbb{R}^4$, $\lambda_s,\ \lambda_r \in \mathbb{R}^2$ are the inductor fluxes in dq-coordinates (stator and rotor respectively), $x_m = J_m\omega_r$ is the mechanical Hamiltonian variable, ω_r the angular speed of the rotor, and J_m is the total moment of inertia of the rotating parts. The structure $\mathcal{J}_D \in \mathbb{R}^{5\times5}$ and damping $\mathcal{R}_D \in \mathbb{R}^{5\times5}$ matrices are

$$\mathcal{J}_D = \begin{pmatrix} -\omega_s L_s J_2 & -\omega_s L_{sr} J_2 & O_{2\times1} \\ -\omega_s L_{sr} J_2 & -(\omega_s - \omega_r) L_r J_2 & L_{sr} J_2 i_s \\ O_{1\times2} & L_{sr} i_s^T J_2 & 0 \end{pmatrix}$$

$$\mathcal{R}_D = \begin{pmatrix} R_s I_2 & O_{2\times2} & O_{2\times1} \\ O_{2\times2} & R_r I_2 & O_{2\times1} \\ O_{1\times2} & O_{1\times2} & B_r \end{pmatrix},$$

where L are inductances, R are resistances, lower indices s and r refer to stator and rotor respectively, B_r is the mechanical damping, i_s and $i_r \in \mathbb{R}^2$ are the stator and rotor currents and

$$J_2 = \begin{pmatrix} 0 & -1 \\ 1 & 0 \end{pmatrix} \in \mathbb{R}^{2\times2} \qquad I_2 = \begin{pmatrix} 1 & 0 \\ 0 & 1 \end{pmatrix} \in \mathbb{R}^{2\times2}. \tag{2}$$

Currents $i^T = (i_s^T, i_r^T) \in \mathbb{R}^4$ and fluxes Λ are related by $\Lambda = \mathcal{L}i$, where the inductance matrix $\mathcal{L}$ is

$$\mathcal{L} = \begin{pmatrix} L_s I_2 & L_{sr} I_2 \\ L_{sr} I_2 & L_r I_2 \end{pmatrix} \in \mathbb{R}^{4\times4}.$$

The interconnection matrix is

$$g_D = \begin{pmatrix} I_2 & O_{2\times2} \\ O_{2\times2} & I_2 \\ O_{1\times2} & O_{1\times2} \end{pmatrix} \in \mathbb{R}^{5\times4}$$

with the port variables $u^T = (v_s^T, v_r^T) \in \mathbb{R}^4$, where $v_s,\ v_r \in \mathbb{R}^2$ are the stator and rotor voltages. Finally, the Hamiltonian function is

$$H_D = \frac{1}{2}\Lambda^T \mathcal{L}^{-1} \Lambda + \frac{1}{2J_m} x_m^2.$$

2.2 The back-to-back converter

Fig. 3 shows the back-to-back converter selected for this system. It is made of a full bridge AC/DC single-phase boost-like rectifier and a 3-phase DC/AC inverter. The whole converter has an AC single-phase voltage input and its output are 3-phase PWM voltages which feed the rotor windings of the electrical machine. This system can be split into two parts: a dynamical subsystem (the full bridge rectifier, containing the storage elements), and an static subsystem (the inverter, which, from the energy point of view, acts like a transformer).

$v_i(t) = E\sin(\omega_s t)$ is a single-phase AC voltage source, L is the inductance (including the effect of any transformer in the source), C is the capacitor of the DC part, r takes into

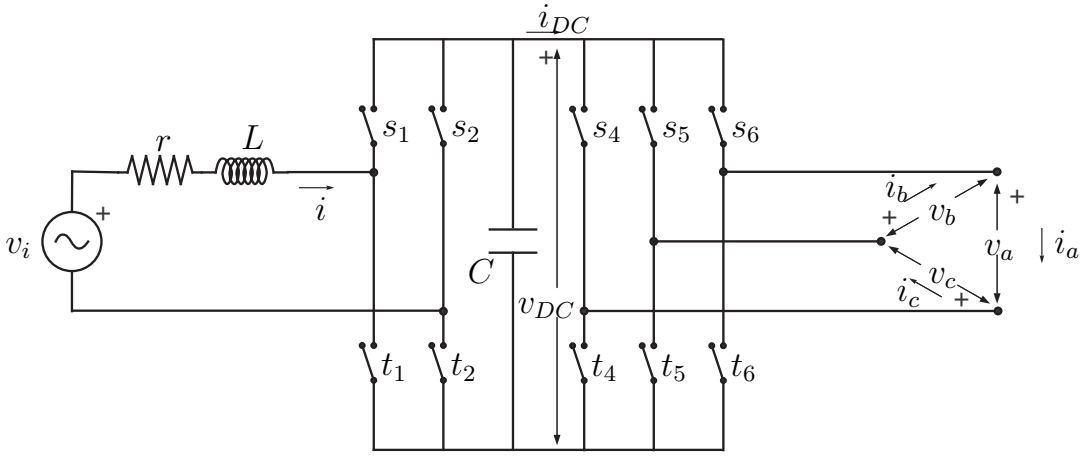

Figure 3: Back-to-back converter.

account all the resistance losses (inductor, source and switches), s_k and t_k, $k = 1, 2, 4, 5, 6$. Switch states take values in $\{-1, 1\}$ and t-switches are complementary to s-switches: $t_k = \bar{s_k} = -s_k$. Additionally, $s_2 = \bar{s_1} = -s_1$.

The PCHS averaged model of the full-bridge rectifier is as follows. The Hamiltonian variables are (B subindex refers to the B2B subsystem) $x_B^T = (\lambda_L, q) \in \mathbb{R}^2$, where λ_L is the inductor flux and q is the DC charge in the capacitor. The Hamiltonian function is

$$H_B = \frac{1}{2L}\lambda^2 + \frac{1}{2C}q^2,$$

while the structure and damping matrices are

$$\mathcal{J}_B = \begin{pmatrix} 0 & -s_1 \\ s_1 & 0 \end{pmatrix} \in \mathbb{R}^{2\times 2} \quad \mathcal{R}_B = \begin{pmatrix} r & 0 \\ 0 & 0 \end{pmatrix} \in \mathbb{R}^{2\times 2}.$$

The interconnection matrix is

$$g_B = \begin{pmatrix} 1 & O_{1\times 3} \\ 0 & f^T \end{pmatrix} \in \mathbb{R}^{2\times 4}, \quad f = \frac{1}{2}\begin{pmatrix} s_6 - s_4 \\ s_5 - s_6 \\ s_4 - s_5 \end{pmatrix} \in \mathbb{R}^3,$$

with inputs

$$u = \begin{pmatrix} v_i \\ -i_{abc} \end{pmatrix} \in \mathbb{R}^4,$$

where $i_{abc}^T = (i_a, i_b, i_c) \in \mathbb{R}^3$ are the three-phase currents in the inverter part. Notice that the inverter subsystem can be seen as a Dirac structure [7] with

$$\begin{aligned} v_{abc} &= f v_{DC} \\ i_{DC} &= f^T i_{abc} \end{aligned}$$

where $v_{abc}^T = (i_a, i_b, i_c) \in \mathbb{R}^3$ are the three-phase voltages and $v_{DC} \in \mathbb{R}$, is the DC voltage, and $i_{DC} \in \mathbb{R}$ is the DC current supplied by the rectifier subsystem.

2.3 The dq-transformation

From an analysis point of view it is convenient to express the three-phase inverter voltages of the DFIM side in dq components.

We can summarize the dq-transformation as follows. First, from the original three phase electrical variables (voltages, currents, fluxes...) y_{ABC} we compute transformed variables $y_{\alpha\beta\gamma}$ by means of $y_{\alpha\beta\gamma} = T y_{ABC}$, with

$$T = \begin{pmatrix} \frac{\sqrt{2}}{\sqrt{3}} & -\frac{1}{\sqrt{6}} & -\frac{1}{\sqrt{6}} \\ 0 & \frac{1}{\sqrt{2}} & -\frac{1}{\sqrt{2}} \\ \frac{1}{\sqrt{3}} & \frac{1}{\sqrt{3}} & \frac{1}{\sqrt{3}} \end{pmatrix},$$

with $T^T = T^{-1}$, so that this is a power–preserving transformation $\langle i, v\rangle = \langle i_{ABC}, v_{ABC}\rangle$. For a three-phase equilibrated system, one has $y_A + y_B + y_C = 0$; the dq-transformation allows then working with only the two first components (the $\alpha - \beta$ components) and neglect the third one, the γ, or homopolar, component, which is zero for any balanced set and which, in any case, is dynamically decoupled from the other components.

The second part of the transformation relies on the assumption that the induction machine is symmetric, with a sinusoidal distribution of magnetic fluxes in the air gap. It eliminates the dependence of the equations on θ (mechanical position of the rotor), and consists in defining new variables y_{dq} via

$$\begin{pmatrix} y_{\alpha\beta s} \\ y_{\alpha\beta r} \end{pmatrix} = K(\theta, \delta) \begin{pmatrix} y_{dqs} \\ y_{dqr} \end{pmatrix} \tag{3}$$

$$K(\theta, \delta) = \begin{bmatrix} e^{J_2\delta} & O_2 \\ O_2 & e^{J_2(\delta-\theta)} \end{bmatrix} \in \mathbb{R}^{4\times 4}$$

where δ is an arbitrary function of time, and

$$e^{J_2\phi} = \begin{pmatrix} \cos(\phi) & -\sin(\phi) \\ \sin(\phi) & \cos(\phi) \end{pmatrix} \in \mathbb{R}^{2\times 2}.$$

If $\dot{\delta}$ is the stator frequency ω_s, this has the nice additional property of converting the sinusoidal time-dependent stator variables into constant values, which is useful for controlling purposes [3].

The total $ABC \leftrightarrow dq$ transformation can be seen as a Dirac structure defined by

$$\begin{aligned} v_{ABC} &= K(\theta, \delta) T v_{dq} && (4) \\ i_{dq} &= -(K(\theta, \delta)T)^T i_{ABC}. && (5) \end{aligned}$$

2.4 PCHS model of the whole system

Fig. 4 shows the interconnection scheme of the whole system (B2B+DFIM). The dq-transformation connects the B2B converter with the DFIM as a Dirac structure.

The interconnection relations are

$$\begin{aligned} v_r &= v_{dq} \\ i_r &= i_{dq} \\ v_{ABC} &= v_{abc} \\ i_{ABC} &= i_{abc}. \end{aligned} \tag{6}$$

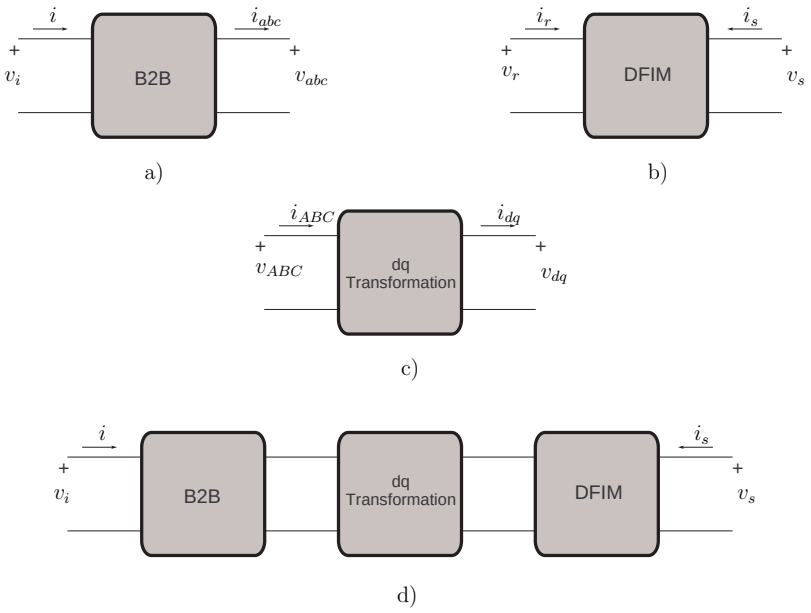

Figure 4: Interconnection scheme.

We use equations (6) and introduce a new $\mathcal{K}$ matrix

$$\mathcal{K} = T_*^T e^{J_2(\delta-\theta)} \in \mathbb{R}^{3\times 2},$$

with T_* defined so as to remove the homopolar component:

$$T_* = \begin{pmatrix} \frac{\sqrt{2}}{\sqrt{3}} & -\frac{1}{\sqrt{6}} & -\frac{1}{\sqrt{6}} \\ 0 & \frac{1}{\sqrt{2}} & -\frac{1}{\sqrt{2}} \end{pmatrix} \in \mathbb{R}^{2\times 3}.$$

The variables of the whole PCHS system are $x^T = (\Lambda^T, J_m\omega_r, \lambda, q) \in \mathbb{R}^7$, with energy function

$$H = H_D + H_B = \frac{1}{2}\Lambda^T\mathcal{L}^{-1}\Lambda + \frac{1}{2J_m}x_m^2 + \frac{1}{2L}\lambda^2 + \frac{1}{2C}q^2.$$

The $\mathbb{R}^{7\times 7}$ structure and dissipation matrices are

$$\mathcal{J}-\mathcal{R} = \begin{pmatrix} & & O_{2\times 1} & O_{2\times 1} \\ \mathcal{J}_D - \mathcal{R}_D & & O_{2\times 1} & \mathcal{K}^T f \\ & & 0 & 0 \\ O_{1\times 2} & O_{1\times 2} & 0 & \\ O_{1\times 2} & -f^T\mathcal{K} & 0 & \mathcal{J}_B - \mathcal{R}_B \end{pmatrix},$$

and the interconnection matrix and port variables are

$$g = \begin{pmatrix} I_2 & O_{2\times 1} \\ O_2 & O_{2\times 1} \\ O_{1\times 2} & 0 \\ O_{1\times 2} & 1 \\ O_{1\times 2} & 0 \end{pmatrix} \in \mathbb{R}^{7\times 3} \qquad u^T = (v_s^T, v_i) \in \mathbb{R}^3.$$

3 Controllers

As mentioned in the Introduction, two controllers were designed for the DFIM an B2B, in [3] and [2] respectively. Both controllers are based on the IDA-PBC method [15]. The central idea is to assign to the closed-loop a desired energy function via modification of the structure and dissipation matrices, still preserving the PCHS structure. That is, the desired target dynamics is a PCHS of the form

$$\dot{x} = (\mathcal{J}_d - \mathcal{R}_d)\nabla H_d \tag{7}$$

where $H_d(x)$ is the new total energy and $\mathcal{J}_d = -\mathcal{J}_d^T$, $\mathcal{R}_d = \mathcal{R}_d^T \geq 0$, are the new structure and damping matrices, respectively. To achieve stabilization of the desired equilibrium point we impose

$$x^* = \arg\min H_d(x).$$

3.1 IDA-PBC controller for a DFIM coupled to a flywheel

In [3] a power flow control strategy was proposed and an IDA-PBC controller was designed for the DFIM . The power management schedule is determined according to the following considerations. The general goal is to supply the required power to the load with a high network power factor, *i.e.*, $Q_n \sim 0$, where Q_n is the network reactive power. On the other hand, it was shown in [3] that the DFIM has an optimal mechanical speed for which there is minimal power injection through the rotor. Combining these two factors suggests to consider the following three modes of operation:

- *(Generator mode*) When the real power required by the local load is bigger than the maximum network power (say, P_n^M) the machine is used as a generator. In this case, the references for the network real and reactive powers are fixed at $P_n^* = P_n^M$ and $Q_n^* = 0$.
- *(Storage mode)* When the local load does not need all the network power and the mechanical speed is far from the optimal value the "unused" network power is employed to accelerate the flywheel. From the control point of view, this operation mode is the same that the *generator mode*; thus the same references are fixed —but now in order to extract the maximum power from the network and to transfer it to the flywheel.
- *(Stand-by mode)* Finally, when the local load does not need all the power network and the mechanical speed is near to the optimal one, the flywheel friction losses are compensated by regulating the speed and the reactive power. Henceforth, the reference for the mechanical speed is fixed at its minimum rotor losses value and $Q_n^* = 0$.

The operation modes boil down to two kinds of control actions (designed as 0 and 1) as expressed in Table 1,[1] where $\epsilon > 0$ is some small pre-assigned error.

[1] In all cases the second reference is $Q_n^* = 0$.

$P_n^* < P_l$	$\lvert\omega_r - \omega_s\rvert \leq \epsilon$	Mode	References
True	True	Generator	$P_n^* = P_n^M$
True	False	Generator	$P_n^* = P_n^M$
False	True	Stand-by	$\omega^* = \omega_s$
False	False	Storage	$P_n^* = P_n^M$

Table 1: Control action table.

The controller obtained with the IDA-PBC procedure is

$$\begin{aligned} v_r &= v_r^* - (\omega_r - \omega^*)(L_r J_2 i_r^* + L_{sr} J_2 i_s) \\ &\quad -L_{sr}\omega^* J_2(i_s - i_s^*) - rI_2(i_r - i_r^*), \end{aligned} \tag{8}$$

where $r > 0$ is a free damping parameter, and $(\cdot)^*$ are the variables values at the desired regulation point. The closed-loop dynamical system takes the form of (7), with

$$\mathcal{J}_{dD} = \begin{pmatrix} -\omega_s L_s J_2 & -\omega_s L_{sr} J_2 & O_{2\times 1} \\ -\omega_s L_{sr} J_2 & -(\omega_s - \omega_r) L_r J_2 & O_{2\times 1} \\ O_{1\times 2} & O_{1\times 2} & 0 \end{pmatrix},$$

$$\mathcal{R}_{dD} = \begin{pmatrix} R_s I_2 & O_2 & O_{2\times 1} \\ O_2 & (R_r + r) I_2 & O_{2\times 1} \\ O_{1\times 2} & O_{1\times 2} & B_r + \xi(x_D) \end{pmatrix},$$

where $\xi(x_D) = \frac{\tau_e^* - \tau_e(\Lambda)}{\omega_r - \omega^*}$, $\tau_e = L_{sr} i_s^T J_2 i_r$ is the electrical torque and $\tau_e^* = B_r \omega_r^*$. With the Hamiltonian function

$$H_{dD} = \frac{1}{2}(\Lambda - \Lambda^*)^T \mathcal{L}^{-1}(\Lambda - \Lambda^*) + \frac{1}{2J_m}(x_m - x_m^*)^2.$$

Standard passiveness arguments apply only to the electrical subsystem, due to the fact that $B_r + \xi(x_D) \geq 0$ is not guaranteed; however, the system has a nice cascade structure and asymptotic stability of overall system follows from well known properties of cascaded systems [3][20].

3.2 IDA-PBC controller for a B2B

An IDA-PBC controller is proposed in [2] for a full-bridge rectifier allowing a bidirectional power flow. The control law is designed using a GSSA model [18] with PCHS structure

$$\mathcal{J} = \begin{pmatrix} 0 & -u_1 & -u_2 \\ u_1 & 0 & \frac{\omega_o L}{2} \\ u_2 & -\frac{\omega_o L}{2} & 0 \end{pmatrix}$$

$$\mathcal{R} = \begin{pmatrix} 0 & 0 & 0 \\ 0 & \frac{r}{2} & 0 \\ 0 & 0 & \frac{r}{2} \end{pmatrix} \quad g = \begin{pmatrix} -1 & 0 \\ 0 & 0 \\ 0 & \frac{1}{2} \end{pmatrix} \quad u = \begin{pmatrix} i_l \sqrt{2x_1} \\ E \end{pmatrix}$$

and Hamiltonian function $H = \frac{1}{C}x_1 + \frac{1}{L}x_2^2 + \frac{1}{L}x_3^2$, where $x_1 = \frac{1}{2}q^2$ ($q = \frac{\langle v_{DC}\rangle_0}{C}$ is the capacitor charge), $x_2 = \frac{\langle i\rangle_1^R}{L}$ and $x_3 = \frac{\langle i\rangle_1^I}{L}$ are the inductor fluxes in GSSA variables ($\langle\cdot\rangle_n$

means the n^{th}-harmonic component), i_l is the load current and u_1, u_2 are the control actions in GSSA variables.

The controller computed with the IDA-PBC method is

$$s = -\frac{2\omega_o x_3^*}{v_{DC}^*}\cos(\omega_o t) + \frac{L i_l}{x_3^*}\sin(\omega_o t)$$

where v_{DC}^* is the desired bus voltage. This yields the following closed-loop structure,

$$\mathcal{J}_{dB} = \begin{pmatrix} 0 & -u_1 & -u_2 \\ u_1 & 0 & \frac{\omega_o L}{2} \\ u_2 & -\frac{\omega_o L}{2} & 0 \end{pmatrix}, \quad \mathcal{R}_{dB} = \begin{pmatrix} 0 & 0 & 0 \\ 0 & \frac{r}{2} & 0 \\ 0 & 0 & \frac{r}{2} \end{pmatrix},$$

with closed-loop energy function

$$H_{dB} = \frac{1}{C}x_1 + \frac{1}{L}x_2^2 + \frac{1}{L}x_3^2 - \frac{2\sqrt{x_1^*}}{C}\sqrt{x_1} - \frac{2}{L}x_3^* x_3. \tag{9}$$

4 Simulations

In this Section we implement a numerical simulation of the whole system controlled via the IDA-PBC. The simulation has been performed using the *20-sim*[2] modelling and simulation software. The parameters used in the simulations are given in Table 2. In order to show a more realistic power flow between the machine, the grid and the load, the parameters are taken from an industrial machine [9]; it differs from the experimental plant of the Geoplex project in that the later is a smaller machine with significant losses.

DFIM	L_{sr}	L_r, L_s	J_m	B_r	R_s	R_r	v_g
Value	0.041	0.042	50.001	0.005	0.087	0.0228	$(380, 0)$

B2B	r	L	C	E
Value	0.08	$1 \cdot 10^{-3}$	$4.5 \cdot 10^{-3}$	68.16

Table 2: Simulation parameter values (in SI units) for the DFIM and the B2B. Additionally, $\omega_s = \omega_o = 2\pi 50$.

A resistive-inductive varying load is simulated. The load is initially $R_l = 1000$, $L_l = 0.01$, changes to $R_l = 1$ at $t = 1$ in 0.05 seconds, and returns to $R_l = 1000$ at $t = 2.45$, also in 0.05 seconds.

For the purposes of testing the controller, a maximum power network of $P_n^M = 10000$ and a desired bus voltage $v_{DC}^* = 150$ have been set. The damping parameter is fixed at $r = 25$.

Figure 5 shows the power required from the load P_l and the active power supplied by the network P_n. Even if P_l is bigger than the maximal power (P_n^M), P_n does not overcome P_n^M. The mechanical speed during the load changes is depicted in Figure 5. Notice that in the stand-by mode ω_r is kept at $\omega_s = 2\pi 50 \frac{rad}{s}$. Figure 6 shows the reactive power compensation of the whole system.

[2]See `www.20sim.com`

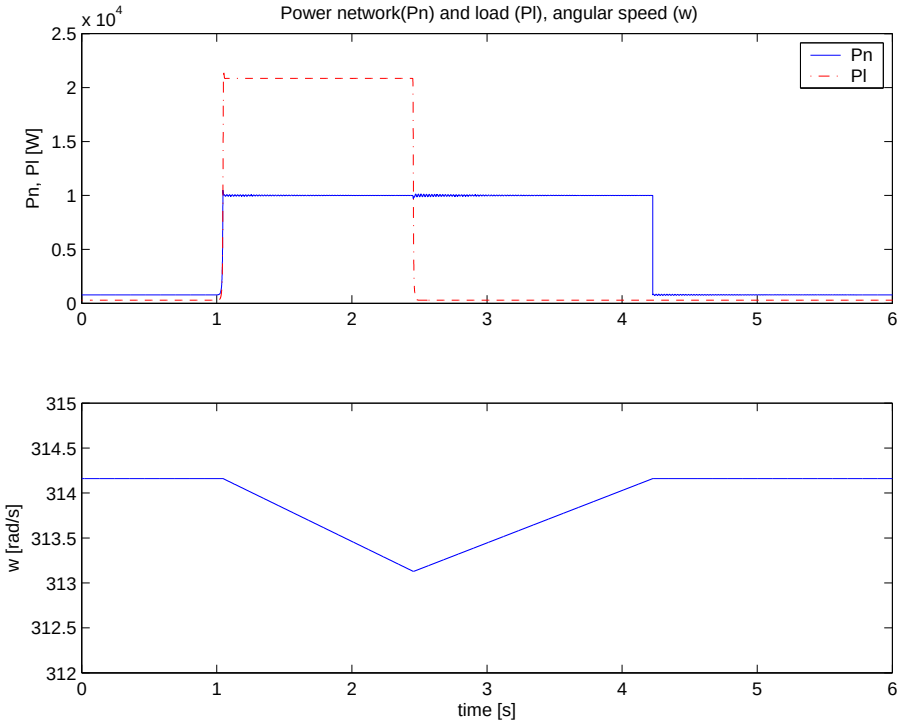

Figure 5: Upper: power network P_n and power load P_l. Lower: mechanical speed ω_r.

Figure 7 shows v_{DC}, which tends v_{DC}^* when the load current i_l (see Figure 8) is constant and remains close to the desired value even in the transient of the machine. Finally, voltage v_i and current i at the single phase source feeding the B2B are depicted in Figure 9, showing that they are nearly in phase.

5 Conclusions

We have modelled and simulated a complex system, with several subsystems from the electric, power electronics and mechanical domains, using the PCHS paradigm. The simulations have been run in closed loop with controllers designed with the IDA-PBC technique developed for port Hamiltonian systems. The description of the whole system as a network of interconnected subsystems which exchange power in a preserving way has proved itself useful both from the modelling and the control specification and design points of view. Experimental validation of the model and controllers is in progress.

References

[1] H. Akagi and H. Sato. Control and performance of a doubly-fed induction machine intended for a flywheel energy storage system. *IEEE Trans. Power Electron.*, (17):109–116, 2002.

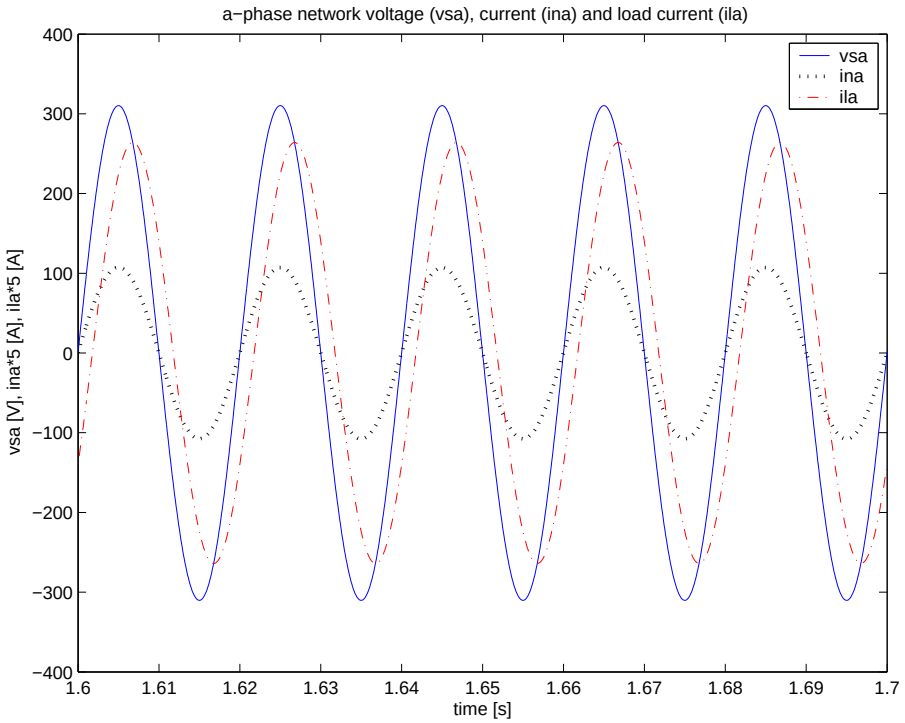

Figure 6: Detail of the grid a-phase voltage v_{sa} and current i_{na}, and load current i_{la}.

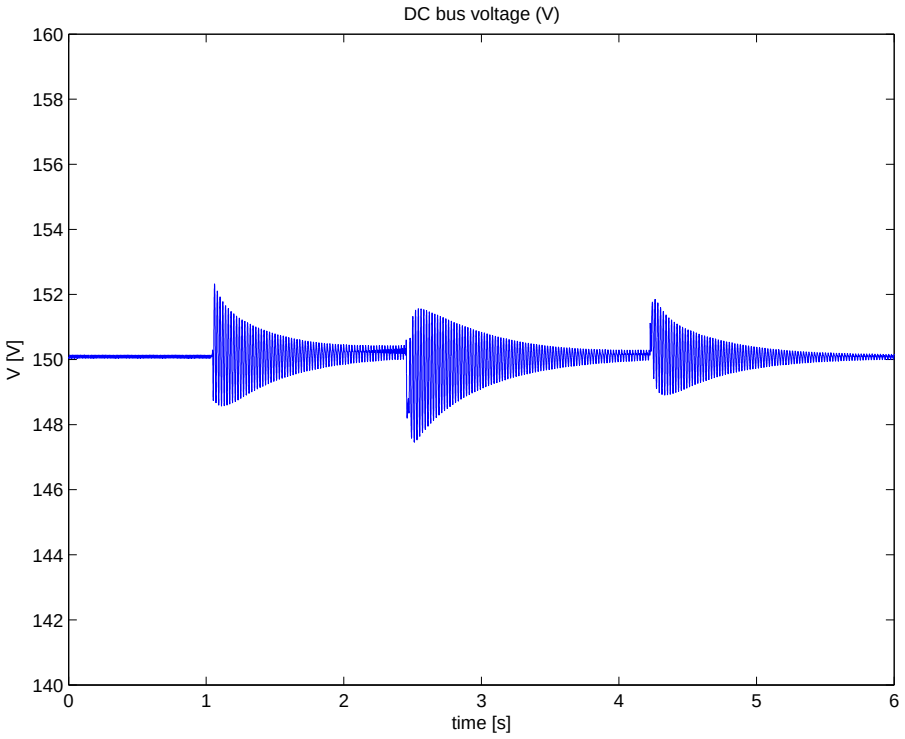

Figure 7: DC-bus voltage v_{DC} of the B2B.

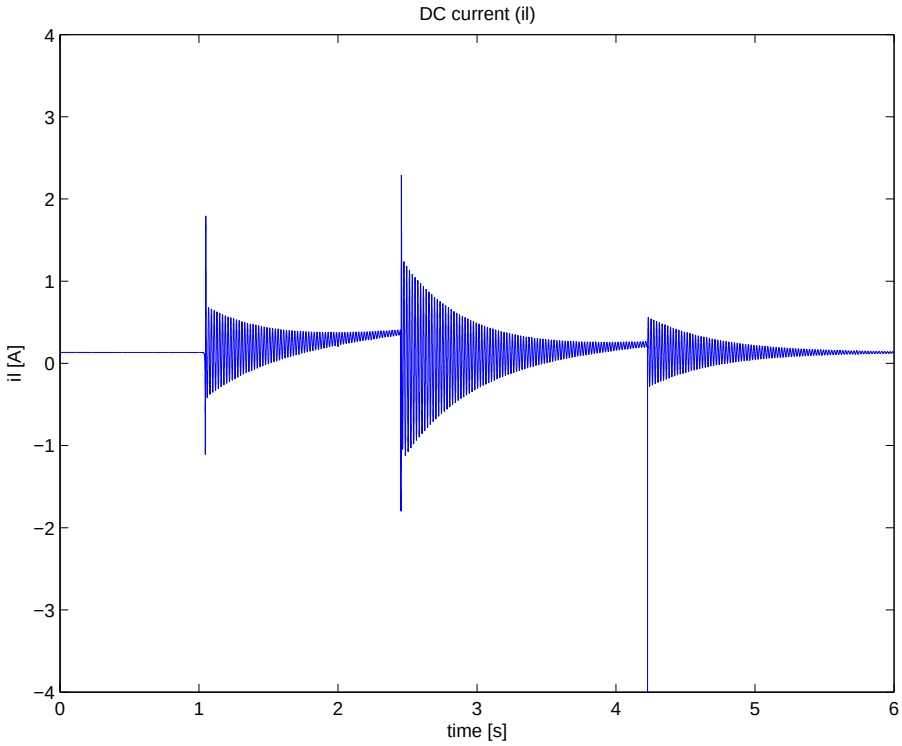

Figure 8: DC load current i_l of the B2B..

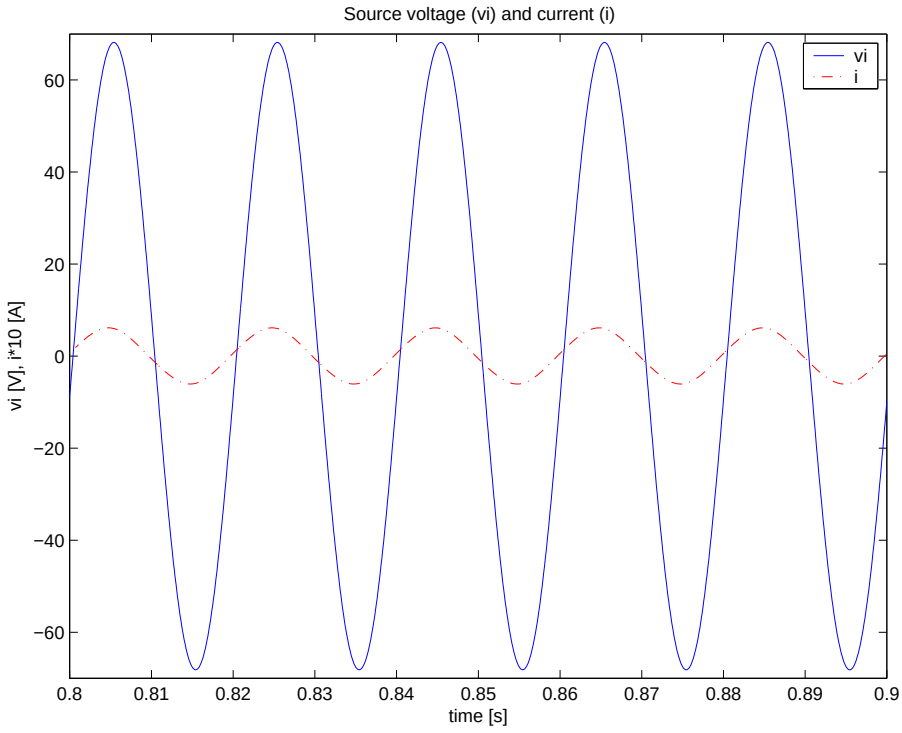

Figure 9: Detail of the AC single-phase voltage and current for the B2B.

[2] C. Batlle, A. Dòria-Cerezo, and E. Fossas. IDA-PBC controller for a bidirectional power flow full-bridge rectifier. In *Submitted to IEEE Proc. Conference on Decision and Control*, 2005.

[3] C. Batlle, A. Dòria-Cerezo, and R. Ortega. Power Flow Control of a Doubly–Fed Induction Machine Coupled to a Flywheel. In *IEEE Proc. Conference on Control Applications*, pages 1645–1651, 2004.

[4] C. Batlle, E. Fossas, R. Griñó, and S. Martínez. Generalized state space averaging for port controlled hamiltonian systems. In *Proc. 16th IFAC World Congress*, 2005.

[5] P.C. Breedveld. MultiBond-graph elements in physical systems theory. *Journal of the Franklin Institute*, 319:1–36, 1985.

[6] P. Caratozzolo, E. Fossas, J. Pedra, and J. Riera. Dynamic modeling of an isolated motion system with DFIG. In *Proc. CIEP*, pages 287–292, 2000.

[7] M. Dalsmo and A. van der Schaft. On representations and integrability of mathematical structures in energy-conserving physical systems. *SIAM J. Control Optim.*, (37):54–91, 1998.

[8] G. Golo, A.J. van der Schaft, P.C. Breedveld, and B. Maschke. Hamiltonian formulation of Bond Graphs. In *Workshop NACO II*, pages 2642–2647, 2001.

[9] P. C. Krause. *Analysis of electric machinery*. McGraw-Hill, 1986.

[10] A. Kugi. *Non-linear control based on physical models*. Springer, 2001.

[11] B. Maschke and A. van der Schaft. Port-controlled Hamiltonian Systems: Modelling origins and system-theoretic properties. In *2nd. IFAC NOLCOS*, pages 282–288, 1992.

[12] B. Maschke and A. van der Schaft. *Systems and networks: Mathematical theory and applications*, volume II, pages 349–352. Academic-Verlag, 1994.

[13] B. Maschke, A. van der Schaft, and P. C. Breedveld. An intrinsic hamiltonian formulation of the dynmics of *lc*-circuits. *IEEE Trans. Circuits and Syst.*, 42:73–82, 1995.

[14] R. Ortega, A. van der Schaft, I. Mareels, and B. Maschke. Putting energy back in control. pages 18–33.

[15] R. Ortega, A. van der Schaft, B. Maschke, and G. Escobar. Interconnection and damping assignment passivity-based control of port-controlled Hamiltonian systems. *Automatica*, (38):585–596, 2002.

[16] R. Peña, J. C. Clare, and G. M. Asher. Doubly fed induction generator using back-to-back pwm converters and its application to variable speed wind-energy generation. In *IEEE Proc. Electric Power Applications*, number 143, pages 231–241, 1996.

[17] S. Peresada, A. Tilli, and A. Tonelli. Power control of a doubly fed induction machine via output feedback. *Control Engineering Practice*, (12):41–57, 2004.

[18] S.R. Sanders, J.M. Noworolski, X.Z. Liu, and G. C. Verghese. Generalized averaging method for power conversion systems. *IEEE Trans. Power Electron.*, 6:251–259, 1991.

[19] J.G. Slootweg, H. Polinder, and W.L. Kling. Dynamic modelling of a wind turbine with doubly fed induction generator. In *IEEE Power Engineering Society Summer Meeting 2001*, pages 644–649, 2001.

[20] E.D. Sontag. A Remark on the Converging-Input Converging-State Property. *IEEE Trans. on Automatic Control*, 48(2):313–314, 2003.

[21] A. van der Schaft. *L_2 gain and passivity techniques in nonlinear control*. Springer, 2000.

[22] A. van der Schaft and B. Maschke. Hamiltonian formulation of distributed-parameter systems with boundary energy flow. *Journal of Geometry and Physics*, 42:166–194, 2002.